Petrology, age, and tectonic setting of the Park Spur pluton, Aspy terrane, central Cape Breton Highlands, Nova Scotia, Canada

Amanda M. Smith, Sandra M. Barr, Chris E. White, Deanne van Rooyen, and Évelyne Sunatori

Department of Earth and Environmental Science, Acadia University, Wolfville Nova Scotia B4P 2R6, Canada
*Corresponding author <sandra.barr@acadiau.ca>

Date received: 25 April 2023 ❡ Date accepted: 28 July 2023

ABSTRACT

The Park Spur pluton was emplaced in the Aspy terrane of the central Cape Breton Highlands at 374.2 ± 2.9 Ma (U–Pb zircon). It consists mainly of muscovite-biotite monzogranite with small areas of garnet-bearing muscovite monzogranite and abundant pegmatite and aplite dykes. On its northern margin the pluton intruded metamorphic rocks of the Ordovician–Silurian Cape North Group and associated orthogneiss and on the south it intruded low-grade metamorphic rocks of the Silurian Calumruadh Brook Formation. Deformation along the southern margin of the Park Spur pluton is consistent with emplacement during dextral transpression between the Bras d'Or and Aspy terranes. The Late Devonian age combined with S-type petrological characteristics show that the Park Spur pluton and nearby Canal pluton are related to the ca. 375 Ma Black Brook Granitic Suite, all interpreted to have been emplaced during later stages of the Acadian orogeny in Ganderia as a result of delamination.

RÉSUMÉ

La mise en place du pluton Park Spur à l'intérieur du terrane Aspy dans le centre des Hautes-Terres-du-Cap-Breton remonte à 374,2 ± 2.9 Ma (datation U–Pb sur zircon). Le pluton est essentiellement constitué de monzogranite à deux micas comportant de petites sections de monzogranite à muscovite grenatifère et une abondance de dykes pegmatitiques et aplitiques. Sur sa bordure septentrionale, le pluton a pénétré des roches métamorphiques du groupe ordovicien-silurien de Cape North et de l'orthogneiss associé, alors qu'il a pénétré au sud des roches faiblement métamorphisées de la Formation silurienne de Calumruadh Brook. La déformation le long de la bordure méridionale du pluton Park Spur correspond à une mise en place durant la transpression dextre survenue entre les terranes Bras d'Or et Aspy. L'âge du Dévonien tardif conjugué aux caractéristiques pétrologiques supracrustales révèle que le pluton Park Spur et le pluton Canal voisin sont apparentés à la suite granitique d'environ 375 Ma du ruisseau Black, tous interprétés comme des éléments s'étant mis en place au cours des stades tardifs de l'orogenèse acadienne dans Ganderia à la suite d'une délamination.

[*Traduit par la redaction*]

INTRODUCTION

The Park Spur pluton (PSP) is located near the eastern edge of the Aspy terrane in the central Cape Breton Highlands, Nova Scotia (Fig. 1). Although the pluton was shown on previous geological maps and assigned an assumed Devonian age (e.g., Jamieson *et al.* 1987; Barr *et al.* 1992), its field relations and composition were poorly constrained because of sparse outcrop in the area, and petrological characteristics and tectonic setting had not been investigated prior to this study. The pluton is of particular interest because it is situated in an area where the orientation of the Eastern Highlands shear zone between the Aspy and Bras d'Or terranes changes trend from northerly to northeasterly (Fig. 1), and where vein-hosted gold mineralization has been linked to Devonian magmatism (e.g., Kontak and Smith 1997; Baldwin 2019). Furthermore, abundant pegmatite associated with the PSP suggests a potential for critical element resources (e.g., Magyarosi 2020).

In recent years new logging roads provided better access to the area and facilitated more detailed mapping and sampling of the PSP and adjacent units. In this paper we report results from that work, focusing on field relations, petrography, geochemistry, and U–Pb zircon dating of the PSP. The new data confirm a Devonian age for the pluton and its petrological similarity to the Black Brook Granitic Suite of the northeastern Aspy terrane (Fig. 1). They also show that the pluton was emplaced in a zone of transpression and rapid exhumation related to juxtaposition of the Aspy and Bras d'Or terranes.

doi:10.4138/atlgeo.2023.007

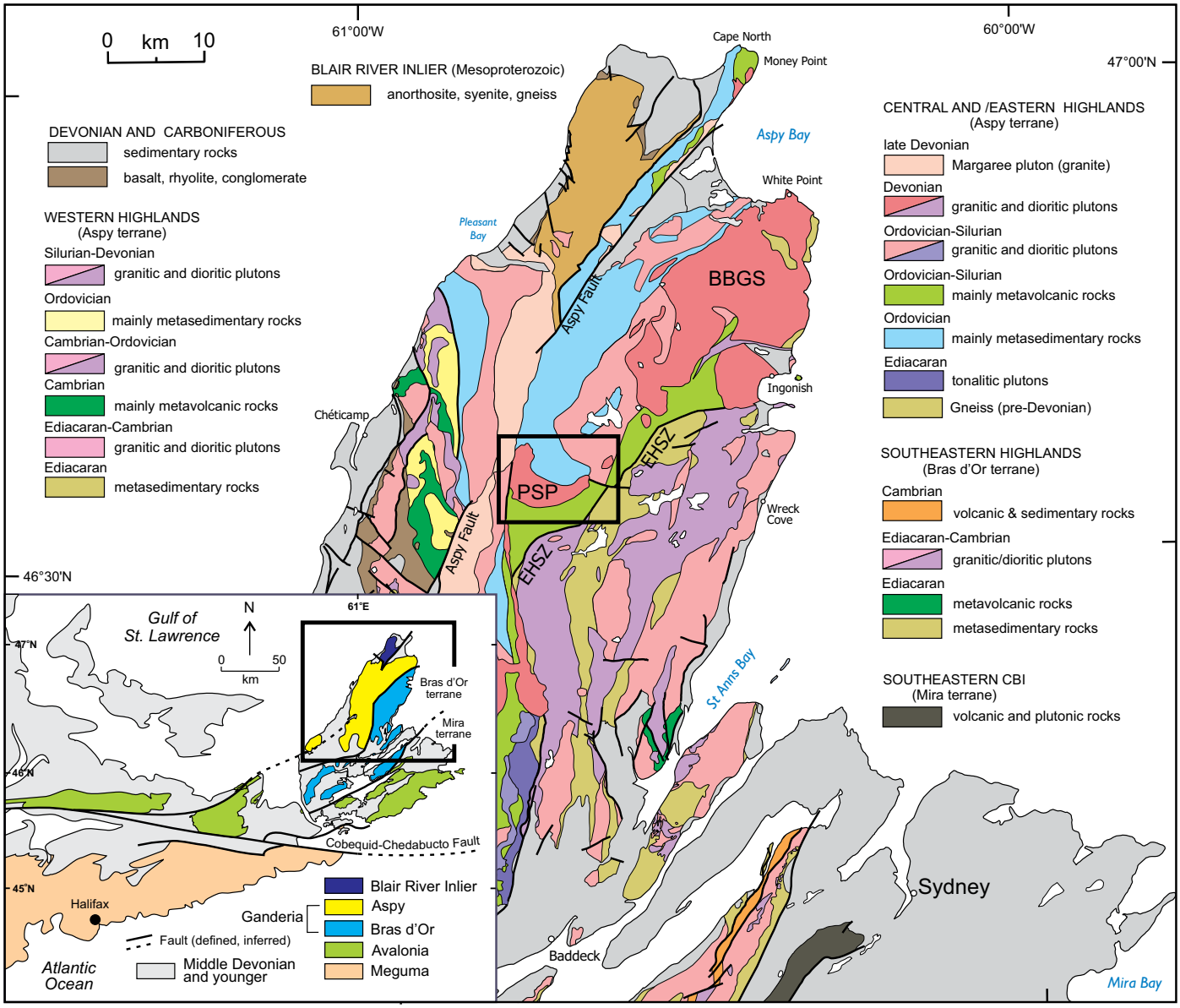

Figure 1. Simplified geological map of northern Cape Breton Island showing major geological components of the Aspy and Bras d'Or terranes and the locations of Figure 2 (black rectangle), Park Spur pluton (PSP), Black Brook Granitic Suite (BBGS), and the Eastern Highlands shear zone (EHSZ) in the central Cape Breton Highlands. Map is modified after White *et al.* (2022). Inset map shows geological components in the eastern Maritime Provinces after Barr *et al.* (2012).

GEOLOGICAL SETTING

Pre-Carboniferous rocks on Cape Breton Island have been divided from north to south into the Blair River inlier and Aspy, Bras d'Or, and Mira terranes (Fig. 1), based on contrasts in geological characteristics (Barr and Raeside 1986, 1989). The Blair River inlier consists mainly of late Mesoproterozoic metamorphic and plutonic rocks and is interpreted to be part of Laurentia (e.g., Miller *et al.* 1996). It is separated from the adjacent Aspy terrane by mylonitic shear zones (e.g., Raeside and Barr 1992). The Aspy terrane contains mainly lower Paleozoic metamorphic and plutonic rocks, separated from the mainly late Neoproterozoic and Cambrian metamorphic and plutonic rocks of the Bras d'Or terrane by the Eastern Highlands shear zone (Fig. 1). Both the Aspy and Bras d'Or terranes are interpreted to be part of Ganderia, telescoped together during the Devonian Acadian orogeny (e.g., Hibbard *et al.* 2006; Lin 1994, 1995; Lin *et al.* 2007; van Staal *et al.* 2021). The Mira terrane south of the Bras d'Or terrane consists mainly of late Neoproterozoic volcanic, sedimentary, and plutonic rocks, overlain by Cambrian sedimentary rocks, and is interpreted to be part of Avalonia (Hibbard *et al.* 2006).

The central part of the Aspy terrane is characterized by a complex assemblage of both low- and high-grade metamorphic rocks of early Paleozoic age (e.g., Barr *et al.* 1992; Barr

and White 2017a, b). They are intruded by Ordovician through Devonian plutonic suites with compositions that include I-type, S-type, and A-type emplaced in volcanic arc, collisional, and extensional settings, respectively (e.g., Barr *et al.* 2018). Recent and on-going work in the Aspy terrane has provided new age constraints and clarified relationships among the metamorphic units (e.g., McCarron 2020; Grant *et al.* 2019; Grant 2020; Piette-Lauzière *et al.* 2018, 2019, in press; Sombini dos Santos *et al.* 2020; Sunatori 2022; White *et al.* 2018). These new interpretations provide a regional context for emplacement of the PSP and other plutonic units (Fig. 1).

FIELD RELATIONS

The PSP is reasonably well represented by outcrops on its northwestern, western, and southern margins, but outcrops are scarce in its central and northern parts (Fig. 2). Hence, the shape of the pluton in those areas has been inferred mainly from geophysical data (e.g., Ethier 2001). Metamorphic rocks in the area north of the PSP were interpreted by Barr *et al.* (1992) to represent undivided Ordovician–Silurian Money Point Group, based on the abundance of mafic rocks such as amphibolite. However, in more recent work by Grant (2020) they were reinterpreted as undivided Cape North Group, consistent with their composition and amphibolite-facies metamorphism. They are intruded by Silurian plutons, now orthogneiss, of the Cheticamp Lake Gneiss (Fig. 2). The intrusive contact of the PSP with amphibolite of the Cape North Group is well exposed in Cheticamp River and related tributaries, where the PSP contains angular banded amphibolite xenoliths. The rest of the northern margin of the PSP is also inferred to be intrusive, although the area is largely obscured by glacial deposits. A small body of granite, referred to here as the Canal pluton because it outcrops along a canal constructed as part of the Wreck Cove Hydroelectric Project, intruded the Cheticamp Lake Gneiss based on mapping by Barr *et al.* (1992). Samples from the Canal pluton are included in the current study (Fig. 2) for comparison with the PSP.

The southern boundary of the PSP is against the Calumruadh Brook Formation (CBF), a new unit described and named informally by Sunatori (2022). The rocks were previously included in the Jumping Brook Metamorphic Suite (Barr *et al.* 1992; Barr and White 2017a, b). The PSP intruded the CBF, based on the presence of granitic and pegmatitic dykes related to the pluton in the CBF and xenoliths of biotite schist from the CBF in the PSP. However, in the western part of the contact zone, both the CBF and adjacent granite of the PSP are mylonitic in the Park Spur Road shear zone (Fig. 2). Foliation is oriented east-west with near-vertical dip parallel to the southern margin of the pluton. Although outcrop is limited in the contact area, some outcrops of the PSP have a down-dip stretching lineation defined by elongate quartz rods, suggesting near-vertical sense of movement between the pluton and country rocks of the CBF. No reliable kinematic indicators were seen, but the difference in grade between the high-grade host rocks at the northern margin of the PSP and low-grade rocks in the CBF along the southern margin (Sunatori 2022) are consistent with upward movement of the pluton relative to the CBF during pluton emplacement.

The Park Spur Road shear zone is terminated on the west by the north-trending Coinneach Brook shear zone (CBSZ). The CBSZ deformed the Silurian Taylors Barren pluton (age 430 ± 2 Ma; Horne *et al.* 2003). It may have also deformed the western edge of the PSP, although that relationship is not constrained by field observations. Both the PSP and the CBSZ were intruded by the Margaree pluton (age ~363 Ma; Sombini dos Santos *et al.* 2020). A cooling age of 372 ± 4 Ma reported by Price *et al.* (1999) from hornblende in amphibolite in the area of the CBSZ is likely dating the time of the last movement on the shear zone, timing corroborated in recent work by Piette-Lauzière (2022) and Piette-Lauzière *et al.* (in press).

PETROGRAPHY

Most of the PSP and the smaller Canal pluton in the Cheticamp Lake Gneiss to the northeast (Fig. 2) consist of medium-grained muscovite-biotite monzogranite. Garnet-bearing muscovite monzogranite forms the northwestern tip of the PSP and a narrow strip along the southwestern margin where it is protomylonitic in the Park Spur Road shear zone (Fig. 2). The muscovite-biotite monzogranite is also protomylonitic in that area and displays porphyroclastic texture and C-S fabric. Variably deformed granitic pegmatite and aplite dykes occur throughout the PSP, and in the CBF in outcrops southeast of the pluton.

Modal compositions of typical samples from the PSP and Canal pluton based on visual estimates using slabs stained for K-feldspar (Hutchinson 1974) plot mainly in the monzogranite field on the IUGS classification diagram (Fig. 3). The average modal composition of the muscovite-biotite monzogranite samples is about 30% quartz, 35% plagioclase, 25% microcline, 7% biotite, 2% muscovite, and 1% opaque and accessory minerals (Smith 2022). Opaque minerals were determined to include both magnetite and ilmenite based on spot checking of opaque minerals during electron microprobe work (Smith 2022). Accessory minerals include zircon, apatite, and rare garnet. Secondary minerals are mainly chlorite, sericite, and minor epidote. Quartz grains are commonly sutured. Microcline displays well defined cross-hatched twinning and contains inclusions of quartz, biotite, and plagioclase, which indicate that microcline formed relatively late in the crystallization sequence. Muscovite interpreted to be of igneous origin occurs as single flakes and clusters of flakes, in places intergrown with biotite. Biotite compositions determined by electron microprobe analysis (Smith 2022) plot on or near the boundary between the fields for biotite in subduction-related calc-alkaline and syn-collisional peraluminous plutons on the

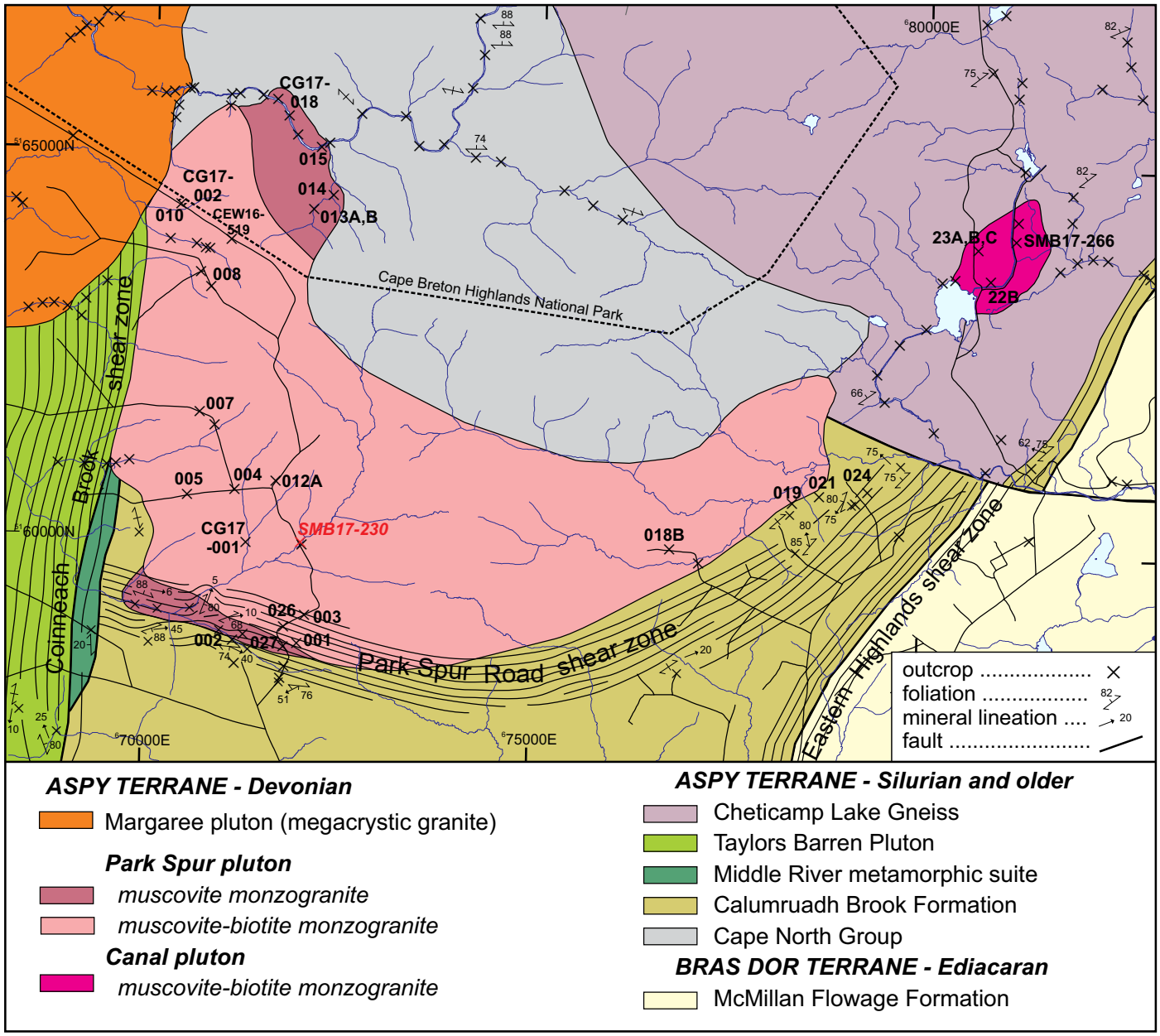

Figure 2. Geologic map of the Park Spur pluton and adjacent units after Smith (2022) and Sunatori (2022). Locations of dated sample SMB17-230 (in red) and other samples used for chemical analysis are shown. Waterways are in blue and roads are thin black lines.

ternary FeO^T-MgO-Al_2O_3 diagram of Abdel-Rahman (1994). Myrmekitic texture is abundant (Fig. 4a), consistent with slow sub-solidus cooling of the rock (e.g., Abart *et al.* 2014). Protomylonitic muscovite-biotite monzogranite in samples from the Park Spur Road shear zone (Fig. 2) have modal compositions similar to the main muscovite-biotite monzogranite to the north, but contain more biotite relative to muscovite, and potassium feldspar grains are larger and form porphyroclasts evident both in hand sample and in thin section (Fig. 4b). These samples have well developed C-S fabric, mortar texture, and ribbon quartz, but myrmekitic texture has been preserved throughout the high-strain zone.

Garnet-bearing muscovite monzogranite is finer grained than the muscovite-biotite monzogranite and has generally higher muscovite and quartz and lower biotite and plagioclase contents (Fig. 3). The average composition based on 4 samples is 35% quartz, 29% microcline, 24% plagioclase, 10% muscovite, 1% biotite, and 1% garnet. Muscovite occurs as large flakes and clusters of flakes (Fig. 4c). Plagioclase is prominently zoned, which together with the finer grain size, suggests more rapid cooling. Small grains of garnet are also present in most samples and compositions determined by electron microprobe analysis are intermediate between alman-

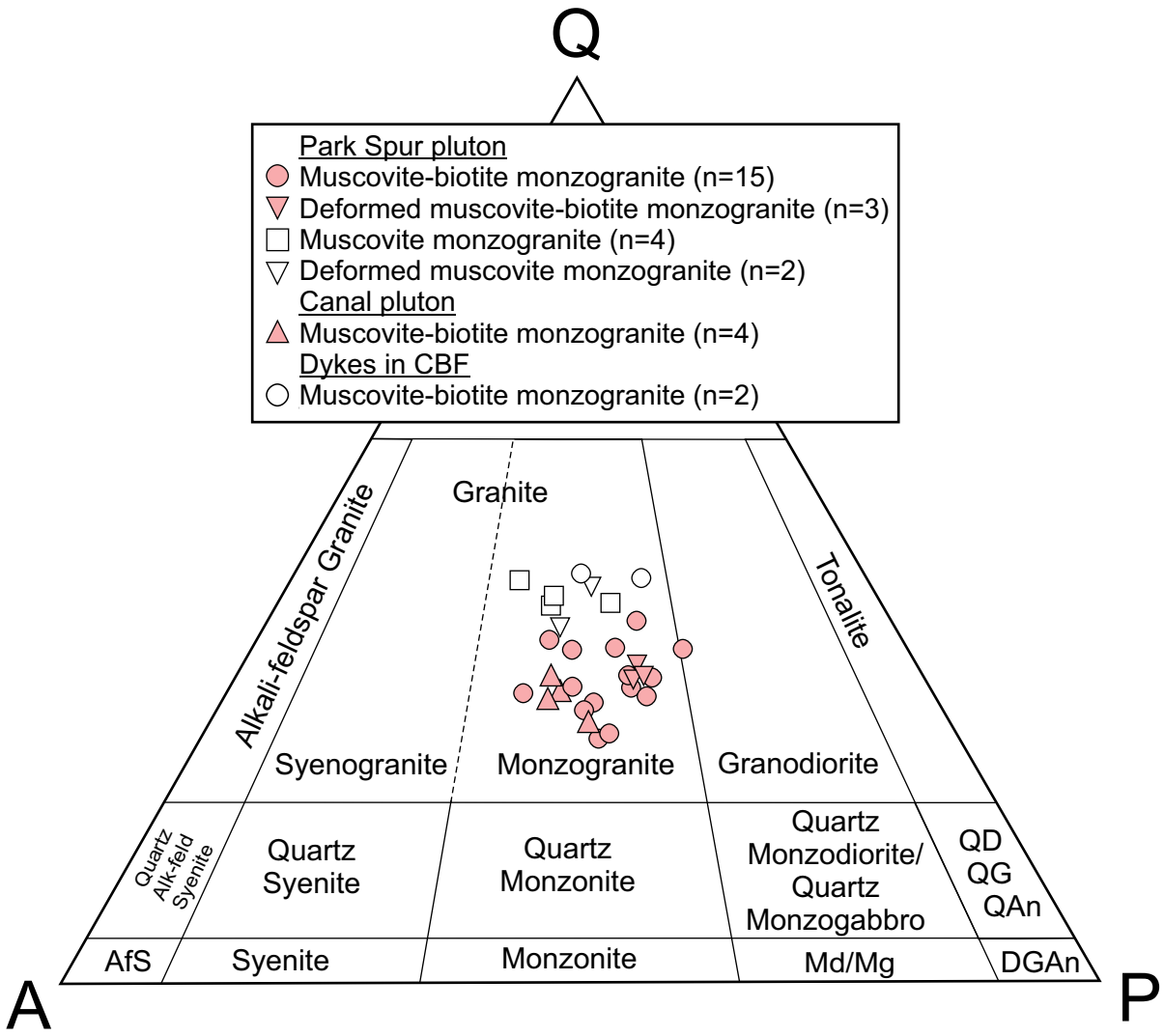

Figure 3. Modal compositions of samples from the Park Spur and Canal plutons plotted on the plutonic rock classification diagram of Streckeisen (1976). Modal compositions were estimated by visual examination of cut slabs stained for K-feldspar (Hutchinson 1974). Abbreviations (ternary endmembers): Q, Quartz; A, Alkali-feldspar, P, Plagioclase; (rock names): AfS, alkali-feldspar syenite; Q, quartz; An, anorthosite; D, diorite; G, gabbro; Md, monzodiorite; Mg, monzogabbro.

dine and spessartine (Smith 2022). Samples from the Park Spur Road shear zone have protomylonitic texture and contain ribbon quartz (Figs. 4b, d).

Pegmatite and associated aplite dykes occur throughout the PSP and Canal pluton. The pegmatite dykes consist mainly of quartz, microcline, plagioclase, and muscovite, minor biotite, and in some places garnet. The aplite dykes contain fine-grained equigranular quartz, microcline, plagioclase, and minor muscovite and biotite.

Muscovite-biotite monzogranite dykes occur rarely in the CBF southeast of the PSP. Two samples have modal compositions similar to the garnet-bearing muscovite monzogranite samples (Fig. 3) but contain both muscovite and biotite and no garnet was observed.

GEOCHRONOLOGY

Methods

Muscovite-biotite monzogranite sample SMB17-230 (Fig. 2) was collected from the PSP for U–Pb zircon dating. The sample was processed by electro-pulse disaggregation and zircon concentrates prepared by conventional methods at Overburden Drilling Management, Ottawa, Ontario. Zircon grains for dating were then hand-selected from the zircon concentrate at Cape Breton University, and selected grains were mounted in an epoxy-covered thin section at the University of New Brunswick, Fredericton, polished to expose the centres of the zircon grains, and imaged using cold cathodoluminescence and back-scattered electron mode to identify textures, internal zoning, and inclusions. These images were used to select ablation points (30 μm diameter),

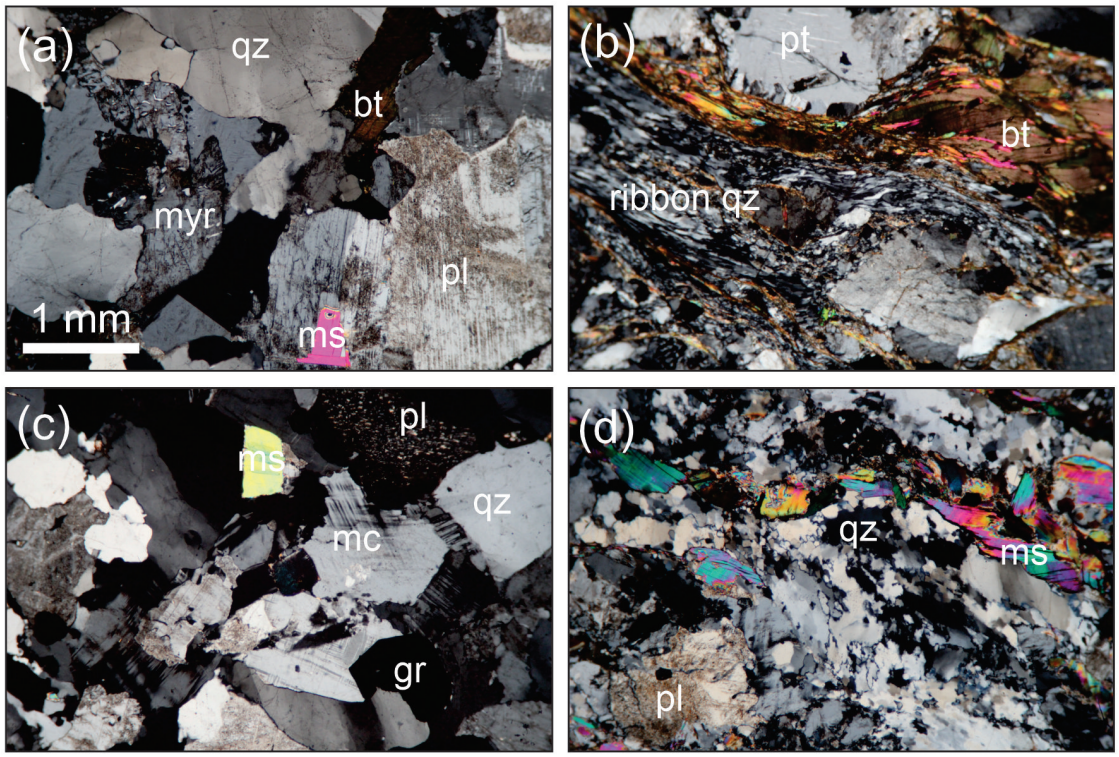

Figure 4. Photomicrographs illustrating minerals and textures in samples from the Park Spur pluton, all with crossed polars. (a) muscovite-biotite monzogranite (sample AS21- 06). (b) deformed muscovite-biotite monzogranite (sample AS21-01). (c) garnet-bearing muscovite monzogranite (sample AS21-15). (d) deformed garnet-bearing muscovite monzogranite (sample AS21-27). Abbreviations: bt, biotite; gr, garnet; mc, microcline; ms, muscovite; myr, myrmekite; pl, plagioclase; pt, perthitic texture in microcline; qz, quartz. Scale bar in (a) applies to all four photomicrographs.

avoiding any visible inclusions, cracks, or other imperfections.

U and Pb isotopes were measured using the Resonetics S-155-LR 193 nm Excimer laser ablation system connected to an Agilent 7700× quadrupole inductively coupled plasma – mass spectrometer in the Department of Earth Sciences at the University of New Brunswick. Analytical procedures followed McFarlane and Luo (2012) and Archibald *et al.* (2013). Data reduction was done using Iolite software (Paton *et al.* 2011) and further reduced for U–Pb geochronology using VizualAge (Petrus and Kamber 2012). VizualAge outputs included uncorrected U–Pb ratios that were used to calculate ^{204}Pb-based corrections (Andersen 2002) and ^{208}Pb-based corrections. Data were filtered using ^{204}Pb as a monitor. For grains with <80 counts/s ^{204}Pb, data are uncorrected; for grains where the percentage error on the ^{204}Pb counts per second was <20%, we used a ^{204}Pb-based correction (Andersen 2002), and for grains where the percentage of radiogenic Pb (PB* in file) is less than 98.5% we used a ^{208}Pb-based correction (Petrus and Kamber 2012). After these corrections were applied, data were sorted by concordance (^{206}Pb/^{238}U versus ^{207}Pb/^{235}U), and by the percentage of radiogenic Pb in the grains as calculated using VizualAge. Analytical data for sample SMB17-230 and isotopic standards are presented in Supplementary Data Table S1.

Results

Data from most of the 35 analyzed zircon grains cluster around concordia at about 350–400 Ma (Fig. 5a). Only one older concordant analysis was obtained at about 600 Ma. The concordia plot in Figure 5a shows the distribution of all the data from this sample. To minimize potential effects of Pb loss on the age, only the 17 grains that are <2% concordant are shown on a probability distribution histogram in Figure 5b which shows a peak at about 375 Ma. The same 17 grains are shown on a concordia diagram in Figure 5c, from which 7 clustered grains with small error ellipses were used to calculate a concordia age of 374.2 ± 2.9 Ma using Isoplot version 4.15 (Ludwig 2012), with 95% confidence and decay-constant errors included in the calculation. Because the MSWD for the calculated concordia age is relatively high, the weighted mean ^{206}Pb/^{238}U age was also calculated using the 14 grains <2% discordant with ages between 400 and 350 Ma (Fig. 5e). It overlaps the calculated concordia age within error, corroborating the interpretation that the concordia age is the best estimate of the crystallization age of the Park Spur pluton. Although it is possible that the older grains represent xenocrystic or inherited grains and that the spread of dates represents complexity in the sample, the analyzed grains display typical oscillatory igneous zoning (Supplementary Data Figure S1) and no differences in Th/U

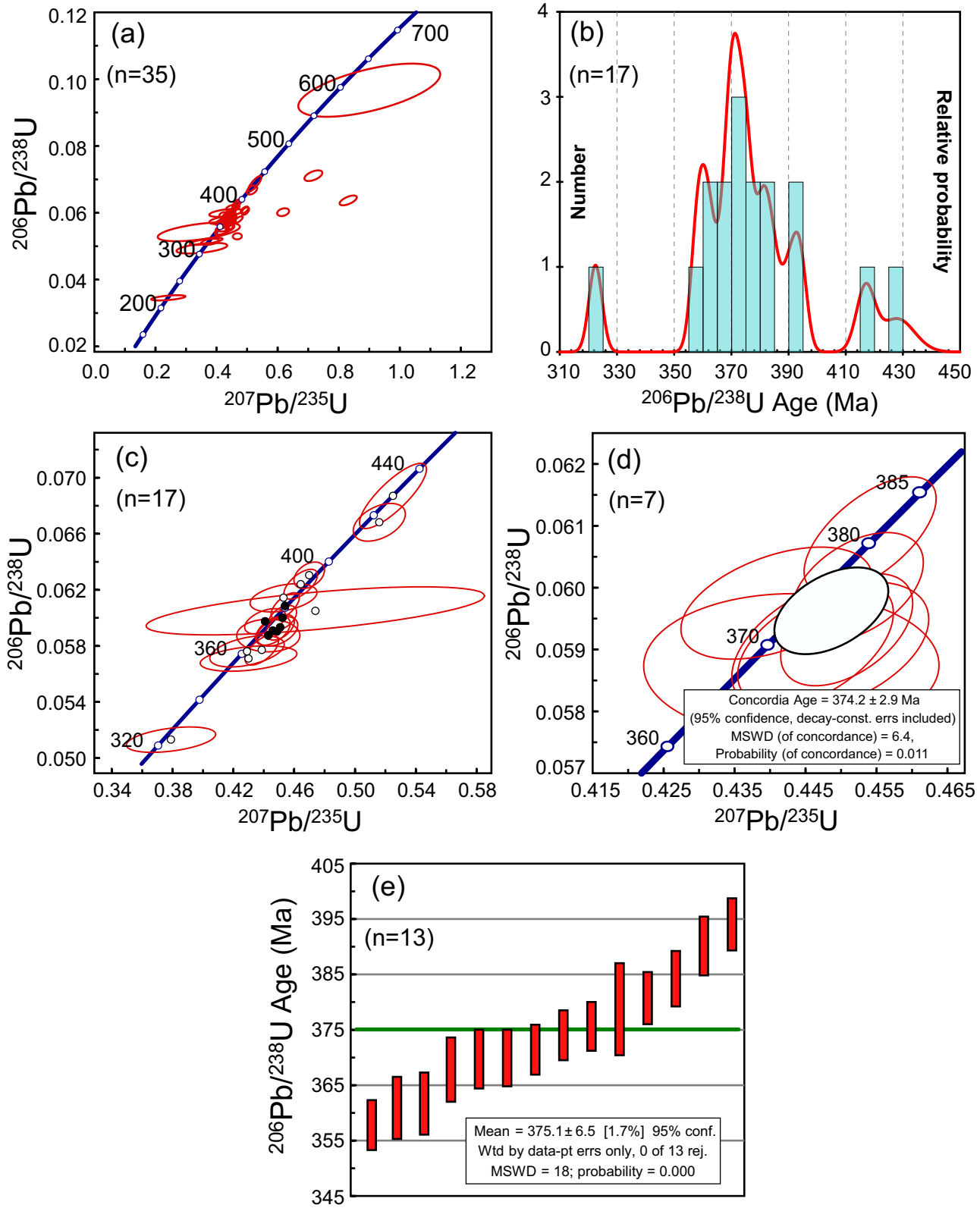

Figure 5. U–Pb zircon data for muscovite-biotite monzogranite sample SMB17-230 from the Park Spur pluton. (a) All data (all error ellipses and box heights are 2σ). (b) Probability distribution of the 17 analyses that are <2% discordant, showing a major peak between 380 and 370 Ma. (c) Concordia plot of 17 grains <2% discordant. The filled black circles indicate the 7 grains that define a cluster of ages around 375 Ma. (d) Concordia age of 374.2 ± 2.9 Ma based on the 7 grains that define the ca. 375 Ma cluster in (c), interpreted to be the best estimate of the igneous crystallization age of the granite. (e) Weighted mean $^{206}Pb/^{238}U$ age of 375.1 ± 6.5 Ma for the 13 grains with ages between 400 Ma and 358 Ma, overlapping the concordia age within error. Data are from Supplementary Data Table S1.

raios to suggest that the older or younger grains are different from the 7 grains used in the concordia calculation (Supplementary Data Table S1). Hence the spread in dates and apparent complexity is more likely an analytical artifact rather than a geologically significant feature of the sample.

This new concordia age is interpreted to be more reliable than the previous concordia age of 379.1 ± 3.5 Ma reported for the PSP by Barr *et al.* (2018), which used only three grains in the concordia age calculation. The new age is within error of the U–Pb zircon TIMS age of 375 +5/-4 Ma reported by Dunning *et al.* (1990) for the Black Brook Granitic Suite (BBGS) and supports earlier assumptions that the PSP and Canal plutons are related to the BBGS.

WHOLE-ROCK GEOCHEMISTRY

Whole-rock chemical data were obtained for 27 samples from the PSP and Canal pluton and associated dykes at Bureau Veritas, Vancouver, BC, using X-ray fluorescence and ICP-MS methods for major elements and trace elements, respectively (Supplementary Data Table S2). In addition, data for 3 samples from the PSP are used from the study by Grant (2018).

The samples have SiO_2 contents between 70% and 75% except for one of the pegmatite dyke samples with 67.9% (Fig. 6). The muscovite-biotite monzogranite samples from the main body of the PSP (n = 14) and Canal pluton (n = 3) range in silica content from about 70% to 74%, whereas the six muscovite monzogranite samples have higher SiO_2, ranging from 74% to 75% (Fig. 6). The two muscovite-biotite monzogranite dyke samples have SiO_2 contents of 73.4 and 74.8%, similar to the muscovite monzogranite samples from the pluton. Four pegmatite and one aplite sample were analyzed for comparison with the other samples and to look for anomalous concentrations of critical elements. Although relatively large (~2 kg) samples were collected, the pegmatite samples show both higher and lower SiO_2 contents than the other samples, likely a "nugget effect" because of their coarse grain size relative to sample size. The aplite sample, on the other hand, is in the centre of the compositional range, with 72.4% SiO_2. Also shown on Figure 6 and subsequent figures for comparison are fields based on previously published analyses from the three units of the Black Brook Granite Suite (BBGS) from the work of Yaowanoiyothin (1988) and Yaowanoiyothin and Barr (1991), as well as three samples from Grant (2018) representing unit 1 (fine- to medium-grained muscovite-biotite monzogranite) and unit 2 (medium- to coarse-grained muscovite-biotite granodiorite to monzogranite) of the BBGS.

Plots of major element oxides (TiO_2, Al_2O_3, Fe_2O_3 (total), MgO, CaO, Na_2O, and K_2O) against SiO_2 are shown to illustrate chemical variations in the samples (Fig. 6). Both MnO and P_2O_5 are close to detection limits (<0.1%) in all samples and hence are not illustrated. The other oxides show scattered but overall negative correlations with SiO_2, except for Na_2O and K_2O which show no systematic variation (Figs. 6a–g). Most samples plot in the high-potassium and shoshonitic fields in the K_2O-SiO_2 diagram (Fig. 6g). No consistent differences are apparent between deformed and undeformed samples of the muscovite-biotite monzogranite and muscovite monzogranite, or between granitic dykes and the samples from the plutons. Samples from the Canal pluton are similar to those from the PSP. Overall, the muscovite-biotite monzogranite samples from the PSP and Canal plutons are most similar to unit 3 (medium-grained muscovite-biotite monzogranite) of the BBGS which forms the southernmost part of the BBGS (Yaowanoiyothin and Barr 1991), whereas the samples from the muscovite monzogranite have higher SiO_2 and are more similar to unit 1 samples from the BBGS (Fig. 6).

Selected trace element variation diagrams are also shown (Figs. 7a–h). Barium, Rb, and Sr substitute for major elements in feldspars, and overall Ba and Sr show negative correlation with SiO_2, whereas Rb shows positive correlation (Figs. 7a–c), but like the major element oxides, they show considerable scatter, especially Rb. Overall, the trends are consistent with variations in the modal abundance of feldspar and quartz in the samples. Zirconium shows negative correlation with SiO_2 whereas Nb and Y show weak positive correlation. The garnet-bearing muscovite monzogranite has highest yttrium content (10–28 ppm). Thorium is generally less than 25 ppm, except in the aplite sample which has 40 ppm (Fig. 7g). Zinc is less than 10 ppm in most samples, but a few have higher abundances, up to 55 ppm in one of the Canal pluton samples (Fig. 7h). The higher Zn and Y shown by the fields for the BBGS samples suggests that the analytical results may be biased toward higher values, although the 3 samples from Grant (2018) also display high Zn (Fig. 7h).

A plot of Zr/Hf ratio against SiO_2 places most of the samples in the field for barren granite, but muscovite monzogranite samples and 3 of the pegmatite samples suggest potential for Sn-W-Mo-Be mineralization associated with greisen-type alteration (Fig. 8a), although none was observed. Based on high alkalis (Na_2O+K_2O) and high SiO_2, the PSP has the most potential for Sn mineralization (Fig. 8b). However, Sn analyses obtained from the samples in this study are less than 2 ppm (Smith 2022).

Muscovite-biotite monzogranite samples from the Park Spur and Canal plutons display similar chondrite-normalized REE patterns, with La enrichment up to 300 times chondritic values (Fig. 9a). Heavy REE are gently sloping to flat at about 2 to 10 times chondritic values. The samples have small negative Eu anomalies, and some samples have small positive Ce anomalies. In contrast, the muscovite monzogranite samples (with one exception) and two muscovite-biotite monzogranite dyke samples are less enriched in light REE (La 20 to 50 times chondritic values), have larger negative Eu anomalies, and display slightly higher heavy REE (Fig. 9b). The REE pattern for the aplite sample is similar to the most light-REE enriched muscovite-biotite monzogranite samples, whereas the pegmatite data are varied but more similar to the muscovite monzogranite

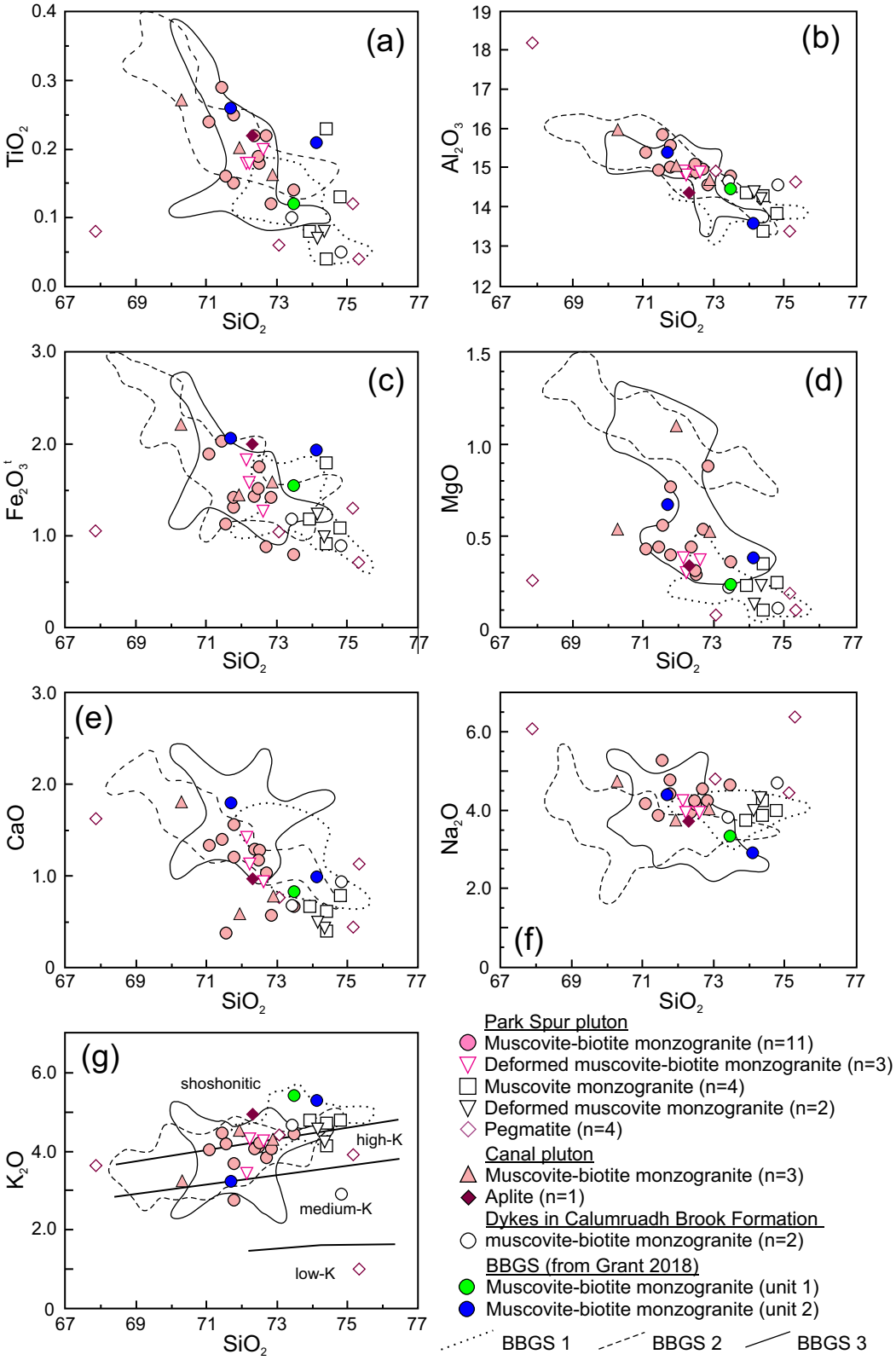

Figure 6. Plots of (a) TiO_2, (b) Al_2O_3, (c) $Fe_2O_3^t$, (d) MgO, (e) CaO, (f) Na_2O, and (g) K_2O against SiO_2. Fields for BBGS 1 to 3 enclose samples from Black Brook Granite Suite unit 1 (fine- to medium-grained muscovite-biotite monzogranite; n = 18), unit 2 (medium- to coarse-grained muscovite-biotite granodiorite to monzogranite; n = 32), and unit 3 (medium-grained muscovite-biotite monzogranite; n = 30) from Yaowanoiyothin (1988) and Yaowanoyothin and Barr (1991). Individual BBGS samples shown on the diagrams are from Grant (2018). Fields in (g) are from Peccerillo and Taylor (1976). Chemical data are listed in Supplementary Data Table S2.

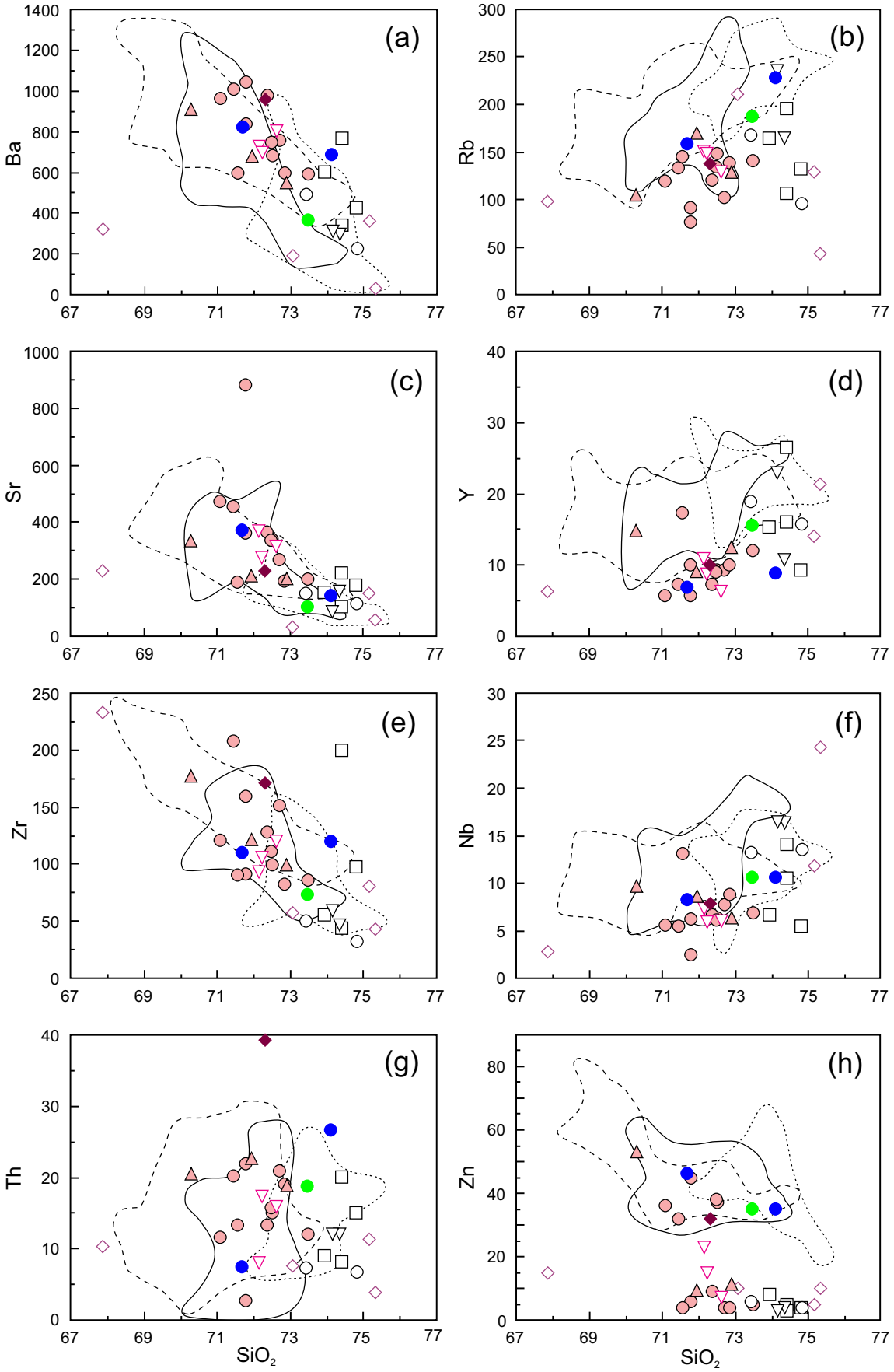

Figure 7. Plots of (a) Ba, (b) Rb, (c) Sr, (d) Y, (e) Zr, (f) Nb, (g) Th, and (h) Zn against SiO_2. Symbols and data sources are as in Figure 6.

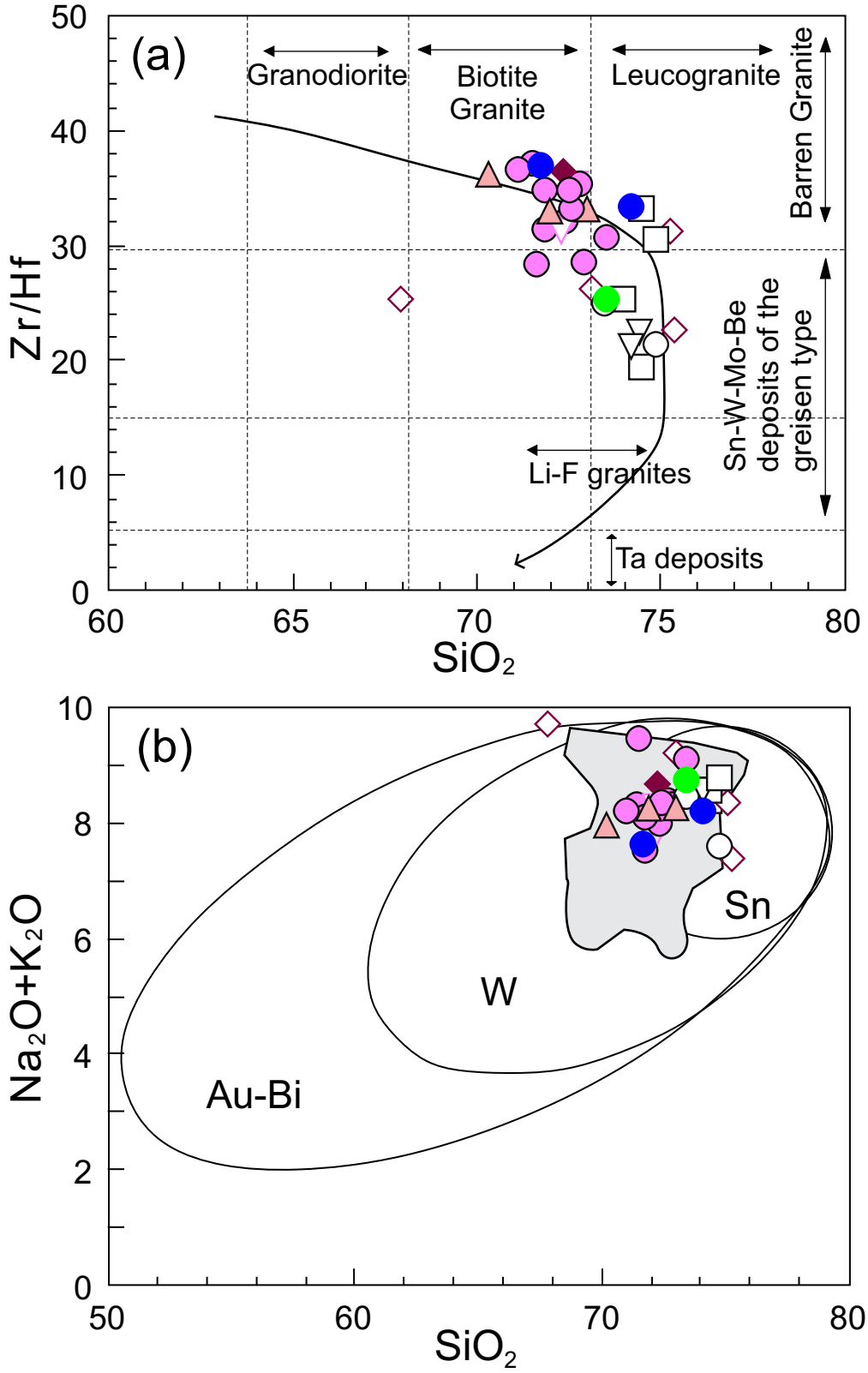

Figure 8. Mineralization potential of granitoid rocks based on (a) Zr/Hf vs SiO_2 and (b) $Na_2O + K_2O$ vs SiO_2. Symbols and data sources are as in Figure 6, except the shaded field in (b) encloses all data from the Black Brook Granitic Suite from Yaowanoiyothin (1988). No Hf data are available for the data from Yaowanoiyothin (1988). Other details on both diagrams are after Azadbakht *et al.* (2019) and Magyarosi (2020).

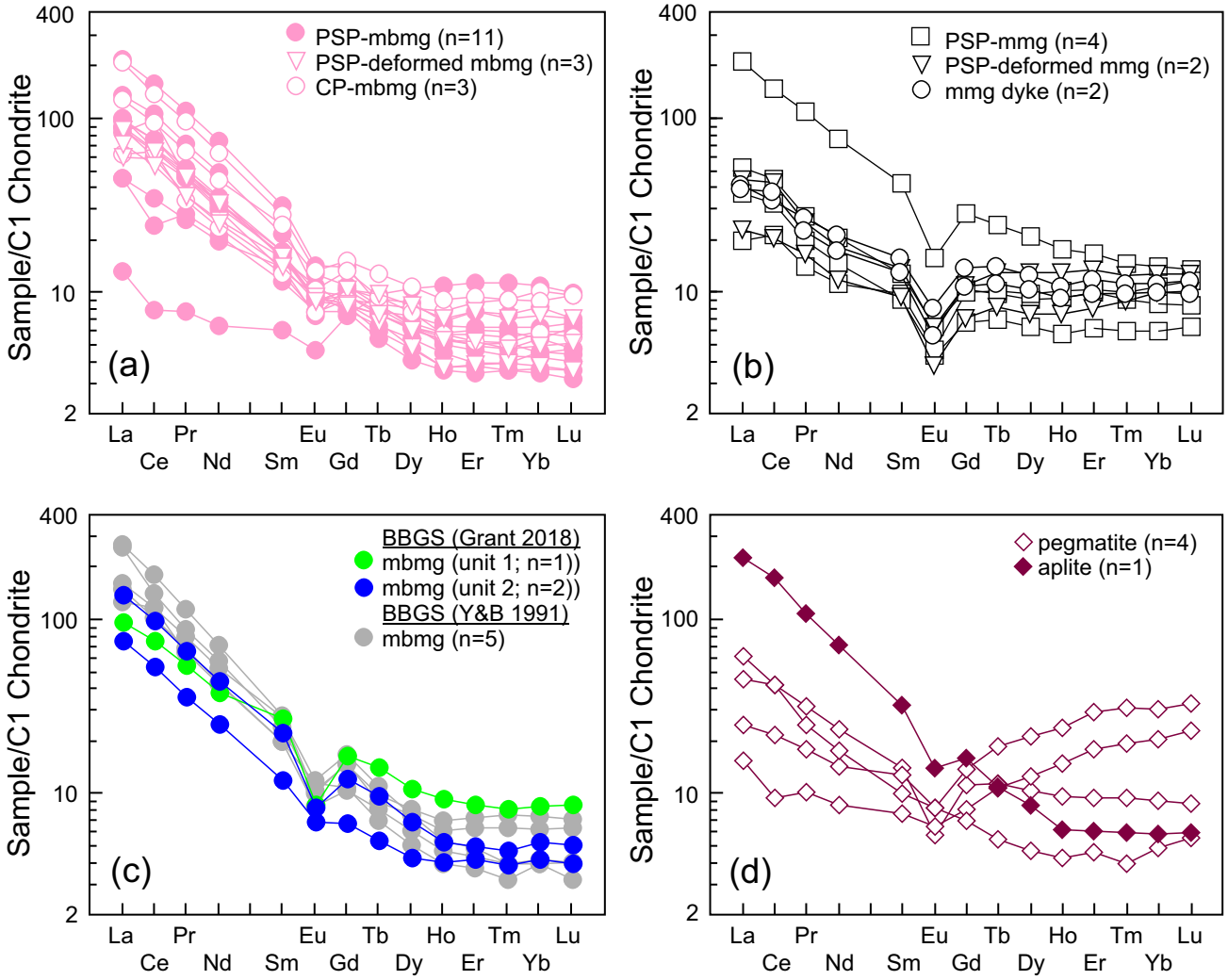

Figure 9. Chondrite-normalized REE data for (a) muscovite-biotite monzogranite, (b) muscovite monzogranite, (c) Black Brook Granitic Suite, and (d) pegmatite and aplite dykes related to the SPP. Chondrite-normalizing values are from Sun and McDonough (1989). Symbols are as in Figure 6, except grey circles in (c) are REE data for selected samples from Black Brook Granitic Suite from Yaowanoiyothin and Barr (1991). Abbreviations: mbmg, muscovite-biotite monzogranite; mmg, muscovite monzogranite; PSP, Park Spur pluton; CP, Canal pluton.

(Fig. 9c). Two pegmatite samples are enriched in heavy REE, likely due to the presence in those two samples of a mineral such as garnet that contains high heavy REE. However, elevated abundances of critical mineral elements were not detected in this study, although lithium was not included in the analyses due to its higher cost.

All samples from the Park Spur and Canal plutons are peraluminous, and most have A/CNK between about 1.05 and 1.35 (Fig. 10a). The samples plot in the overlapping I- and S-type granite fields on diagrams devised by Whalen *et al.* (1987) using Ga/Al ratio to distinguish I- and S-type granites from A-type, such as the Zr versus Ga/Al diagram (Fig. 10b). The presence of primary muscovite combined with A/CNK>1.1 (Fig. 10a) are diagnostic for classification as S-type granite rather than I-type (e.g., Chappell and White 1974). The relatively low Y, Nb, and Rb in these rocks place them in the volcanic-arc granite field on the Rb versus Y + Nb diagram (Fig. 10c). On the Nb versus Y discrimination diagram, most samples plot mainly in the field of slab-failure (break-off) plutons as defined by Hildebrand and Whalen (2014) (Fig. 10d).

DISCUSSION

Comparison to the Black Brook Granitic Suite

Yaowanoiyothin (1988) and Yaowanoiyothin and Barr (1991) divided the Black Brook Granite Suite into 3 units based on texture and modal mineralogy. All three units contain muscovite and biotite but unit 1 contains more muscovite and has the highest average SiO_2 content (74.6%; n = 18), whereas unit 2 is mainly granodiorite (average SiO_2 of 70.9%; n = 32) and unit 3 spans the composition of the other units with an average SiO_2 of 72.2% (n = 31). Based on descriptions by Yaowanoiyothin (1988) and chemical

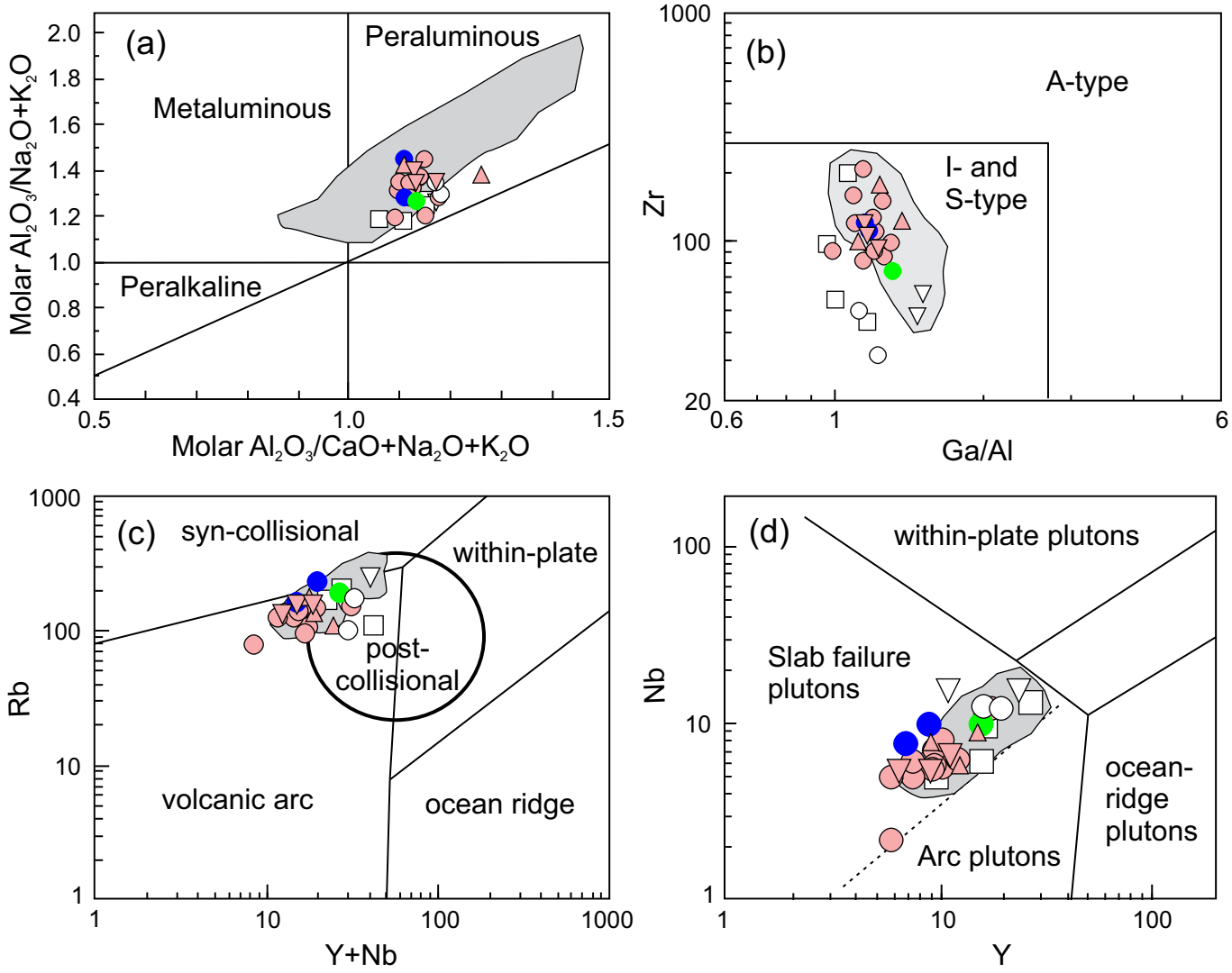

Figure 10. Chemical affinity and tectonic setting classification diagrams for granitoid rocks. (a) Molar $Al_2O_3/(CaO + Na_2O + K_2O)$ against $Al_2O_3/(Na_2O + K_2O)$ with labelled fields from Maniar and Piccolo (1989). S-type granite typically has A/CNK > 1.1 (Chappell and White 1974). (b) Zr (ppm) against Ga/Al with I-, S-, and A-type granite fields after Whalen *et al.* (1987). (c) Rb against Y + Nb with fields from Pearce (1996). (d) Nb versus Y with fields from Pearce *et al.* (1984) and Hildebrand and Whalen (2014). Symbols as in Figure 6, except the shaded field encloses all data from the Black Brook Granitic Suite from Yaowanoiyothin (1988) and Yaowanoyothin and Barr (1991).

characteristics, the Park Spur pluton is most similar to unit 3, which forms the southeastern tip of the BBGS and hence is readily extended into the Canal and Park Spur plutons. Compositional fields for BBGS samples shown on Figures 6 to 10 illustrate the similarity in chemical characteristics between the PSP, Canal pluton, and BBGS. Additional similarities include the presence of abundant pegmatite and aplite in the plutons and adjacent host rocks, as well as the U–Pb zircon ages, which overlap within error.

Yaowanoiyothin and Barr (1991) concluded that compositional variation in the BBGS resulted from fractional crystallization of biotite, plagioclase, microcline, zircon, and apatite from a peraluminous magma derived from a metasedimentary source, interpretations also applicable to the PSP and Canal pluton.

Devonian tectonic setting in the Aspy terrane

The recognition of the Aspy terrane as distinct from Bras d'Or terrane to the south and east was based in part on differences in petrological characteristics of their plutonic components juxtaposed at the Eastern Highlands shear zone (Barr and Raeside 1986, 1989). Decades of subsequent work has confirmed this distinction, now supported by U–Pb zircon ages which demonstrate that the plutonic rocks of the Aspy terrane in the central and eastern Cape Breton Highlands are mainly Silurian and Devonian in contrast to late Ediacaran–Cambrian magmatism in the Bras d'Or terrane (e.g., Barr *et al.* 2018; this study). It is now also recognized that rocks formed at different crustal levels have been juxtaposed along major shear zones within the Aspy terrane,

and not just at its boundary with the Bras d'Or terrane. The BBGS and PSP were emplaced at mesozonal depth, based on the presence of magmatic muscovite and myrmekitic texture, into high-grade metamorphic rocks with both igneous and sedimentary protoliths of Ordovician, Silurian, and early Devonian age metamorphosed and deformed in older subduction zones (e.g., McCarron 2020; Grant 2020). In contrast, large areas of the Aspy terrane contain lower metamorphic grade sedimentary and volcanic rocks formed in Silurian to early Devonian subduction settings (e.g., Barr and Jamieson 1991; Barr *et al.* 2018; White *et al.* 2018). The original relationship among these contrasting low- and high-grade areas is not yet clear, but activation and reactivation of major shear zones within the Aspy terrane has clearly played a major role (e.g., Piette-Lauzière 2022; Sunatori 2022; this study).

On its northern margin the PSP intruded high-grade Ordovician–Silurian metamorphic rocks of the Cape North Group at mesozonal depth (>10 km). Based on its age and deformation fabrics, on its southern margin the pluton was emplaced synchronously with movement on the east-west-trending Park Spur Road shear zone and juxtaposed in a southerly direction over the low-grade metasedimentary and metavolcanic rocks of the Ordovician–Silurian Calumruadh Brook Formation. Ongoing dextral transpression between Aspy and Bras d'Or terranes on the Eastern Highlands shear zone reactivated the north-south-trending Coinneach Brook shear zone, on which the higher-grade Middle River metamorphic suite and Silurian Taylors Barren pluton farther west within the Aspy terrane were transported upward relative to the adjacent CBF and PSP (Sunatori 2022; Piette-Lauzière 2022). By about 365 Ma, convergence had mainly ended, as evidenced by shallow emplacement of the ca. 363 Ma Margaree pluton into these shear zones in an extensional setting (Sombini dos Santos *et al.* 2020).

Hence earlier interpretations (e.g., Price *et al.* 1999; Lin *et al.* 2007; Grant 2020) which viewed the Aspy terrane more simply as a Silurian volcanic arc built on Bras d'Or terrane crust but separated from the Bras d'Or terrane by a back-arc basin that closed in the Devonian, are too simplistic. The Aspy terrane likely contains crustal fragments representing earlier parts of the complex history of Ganderia seen in central Newfoundland and New Brunswick, but both compressed and extended, as well as laterally transported along major shear zones (Waldron *et al.* 2015; van Staal *et al.* 2021), reactivated by the oblique collision of the Meguma terrane outboard of Avalonia (e.g., Piette-Lauzière 2022).

Widespread Silurian and Devonian plutons are characteristic of Ganderia in the northern Appalachian orogen and are generally attributed to the late Silurian–early Devonian (421–400 Ma) Acadian orogeny, brought about by collision of Avalonia with Ganderia (e.g., van Staal *et al.* 2009, 2021). The large volume of plutons both along strike and across strike in Ganderia has been attributed to continuing flat-slab subduction and delamination of the Avalonian plate under Ganderia after collision, culminating in slab failure at about 400 Ma (e.g., van Staal *et al.* 2009, 2021; van Staal and Barr 2012). However, voluminous plutonism also continues into the Middle and Late Devonian in Ganderia and has been referred to as late Acadian (e.g., Gibson *et al.* 2021) or Neoacadian (van Staal *et al.* 2009). The Park Spur and Canal plutons, as well as the Black Brook Granite Suite, are examples of these late Acadian/Neoacadian plutons. They have chemical characteristics of S-type granite plutons formed in a collisional to post-collisional tectonic settings and associated with slab failure (Figs. 10a–d). The tectonic model for Neoacadian shear zone reactivation in the northern Appalachian orogen proposed by Piette-Lauzière (2022) and Piette-Lauzière *et al.* (in press) provides a possible mechanism for magma formation under Ganderia at ca. 375 Ma through crustal-scale shear zones that brought asthenospheric mantle against the lower crust. Although slab failure is indicated for these plutons (Fig. 10d), it may be that the discrimination diagram does not distinguish between delamination and slab failure. Slab failure at 375 Ma is less feasible because subduction continued into the Carboniferous to bring the Gondwanan continents into composite Laurentia during the Alleghenian orogeny, although localized slab failure may have occurred.

The Bras d'Or terrane was not intruded by the Devonian plutons that dominate the Aspy terrane (such as PSP and BBGS) nor was it affected by the pervasive Devonian deformation and metamorphism evident in the Aspy terrane, as confirmed by U–Pb zircon dating (van Rooyen and Barr 2020, 2022) which yielded Neoproterozoic ages from granitic plutons in the adjacent Bras d'Or terrane suggested previously to be Devonian (Kontak and Smith 1997).

CONCLUSIONS

Mapping and petrological studies have resulted in improved understanding of the Park Spur pluton and adjacent units. The PSP and smaller Canal pluton to the northeast have been shown to consist mainly of muscovite-biotite monzogranite like that in the Black Brook Granitic Suite. Garnet-bearing muscovite monzogranite is a minor component at the northwestern tip of the pluton and along the southwestern edge. Granitic pegmatite and aplite dykes occur throughout the PSP and Canal pluton. The presence of xenoliths of amphibolite in the northwestern part of the PSP confirm its intrusive contact with amphibolitic host rocks of the Ordovician–Silurian Cape North Group on the north. Along its southern margin the PSP is deformed in the Park Spur Road shear zone which merges to the east with the Eastern Highlands shear zone. However, that contact is inferred to have been originally intrusive based on the presence of granitic dykes and pegmatite in the Calumruadh Brook Formation, but based on age, synchronous with shear zone deformation.

All components of the PSP are peraluminous and have the overall textural, mineralogical, and chemical characteristics of "S-type" granite. The abundance of myrmekitic texture and igneous muscovite are consistent with mesozonal

emplacement (6–15 km depth). As in the related Black Brook Granitic Suite, chemical variations in the PSP may be related to crystal fractionation of K-feldspar, and to a lesser extent the combined fractionation of plagioclase and biotite. Based on tectonic setting discrimination diagrams using chemical characteristics, the PSP and other S-type plutons of similar age may have formed as a result of crustal-scale shear zones that brought asthenospheric mantle to relatively shallow depth under part of the Aspy terrane.

ACKNOWLEDGEMENTS

This work was funded by a Co-operative Education In-centive Agreement and Mining Industry Human Resources Council "Gearing Up" wage subsidy to support the honours thesis project of Amanda Smith. It was also supported by NSERC Discovery Grant 2016-A4280 to Sandra Barr. Data generated during this study are available in the BSc Honours thesis by Amanda Smith in the library archives at Acadia University. We thank David West and an anonymous journal reviewer for their thorough and insightful reviews which significantly improved the manuscript.

URL LINKS TO SUPPLEMENTARY DATA

Supplementary Data Table S1: https://journals.lib.unb.ca/index.php/ag/article/view/33428/1882529101
Supplementary Data Figure S1: https://journals.lib.unb.ca/index.php/ag/article/view/33428/1882529098
Supplementary Data Table S2: https://journals.lib.unb.ca/index.php/ag/article/view/33428/1882529099

REFERENCES

Abart, R., Heuser, D., and Habler G. 2014. Mechanisms of myrmekite formation: case study from the Weinsberg granite, Moldanubian zone, Upper Austria. Contributions to Mineralogy and Petrology, 168, pp. 1–15. https://doi.org/10.1007/s00410-014-1074-7

Abdel-Rahman, A.M. 1994. Nature of biotites from alkaline, calc-alkaline, and peraluminous magmas. Journal of Petrology, 35, pp. 525–541. https://doi.org/10.1093/petrology/35.2.525

Anderson, T. 2002. Correction of common lead in U–Pb analyses that do not report 204Pb. Chemical Geology, 192, pp. 59–79. https://doi.org/10.1016/S0009-2541(02)00195-X

Archibald, D.B., Barr, S.M., Murphy, J.B., White, C.E., MacHattie, T.G., Escarraga, E.A., Hamilton, M.A., and McFarlane, C.R.M. 2013. Field relationships, petrology, age, and tectonic setting of the Ordovician West Barneys River Plutonic Suite, southern Antigonish Highlands, Nova Scotia, Canada. Canadian Journal of Earth Sciences, 50, pp. 727–745. https://doi.org/10.1139/cjes-2012-0158

Azadbakht, Z., Rogers, N., Lentz, D.R. and McFarlane, C.R.M., 2019. Petrogenesis and associated mineralization of Acadian related granitoids in New Brunswick. *In* Targeted Geoscience Initiative: 2018 report of activities. *Edited by* N. Rogers. Geological Survey of Canada, Open File 8549, p. 243–278. https://doi.org/10.4095/313658

Baldwin, G. 2019. The Highlands Gold occurrences, eastern Cape Breton Highlands, Nova Scotia: an unrecognized IOCG district? Abstract in Abstracts, GAC-MAC-IAH Joint Annual Meeting, Quebec City, May 12–15, p. 58.

Barr, S. M. and Jamieson, R. A. 1991. Tectonic setting and regional correlation of Ordovician– Silurian rocks of the Aspy terrane, Cape Breton Island, Nova Scotia. Canadian Journal of Earth Sciences, 28, pp. 1769–1779. https://doi.org/10.1139/e91-158

Barr, S.M. and Raeside, R.P. 1986. Pre-Carboniferous tectonostratigraphic subdivisions of Cape Breton Island, Nova Scotia. Maritime Sediments and Atlantic Geology, 22, pp. 252–263. https://doi.org/10.4138/1610

Barr, S. M. and Raeside, R. P. 1989. Tectono-stratigraphic terranes in Cape Breton Island, Nova Scotia: implications for the configuration of the northern Appalachian orogen. Geology, 17, pp. 822–825. https://doi.org/10.1130/0091-7613(1989)017<0822:TSTICB>2.3.CO;2

Barr, S.M. and White, C.E. 2017a. Bedrock geology map of the Cheticamp River area, NTS 11K/10, Inverness and Victoria Counties, Nova Scotia. Nova Scotia Department of Natural Resources, Geoscience and Mines Branch. Open File Map ME 2017-026, scale 1:50 000, 1 sheet.

Barr, S. M. and White, C. E. 2017b. Bedrock geology legend for Cape Breton Island, Nova Scotia; Nova Scotia Department of Natural Resources, Geoscience and Mines Branch, Open File Illustration ME 2017-001.

Barr, S.M., Jamieson, R.A., and Raeside, R.P. 1992. Northern Cape Breton Island. Department of Energy, Mines and Resources Canada. Geological Survey of Canada Map 1752A, scale 1:100 000, 1 sheet.

Barr, S.M., White, C.E., and Ketchum, J.W.F. 2012. The Cape Porcupine Complex, northern mainland Nova Scotia – no longer a geological orphan. Atlantic Geology, 48, pp. 70–85. https://doi.org/10.4138/atlgeol.2012.004

Barr, S.M., van Rooyen, D., and White, C.E. 2018. Granitoid plutons in peri-Gondwanan terranes of Cape Breton Island, Nova Scotia, Canada: new U–Pb (zircon) age constraints. Atlantic Geology, 54, pp. 21–80. https://doi.org/10.4138/atlgeol.2018.002

Chappell, B.W. and White, A.J.R. 1974. Two contrasting granite types. Pacific Geology, 8, pp. 173–174.

Dunning, G.R., Barr, S.M., Raeside, R.P., and Jamieson, R.A. 1990. U–Pb zircon, titanite, and monazite ages in the Bras d'Or and Aspy terranes of Cape Breton Island, Nova Scotia: Implications for igneous and metamorphic history. Geological Association of America Bulletin 102, pp. 322–330. https://doi.org/10.1130/0016-7606(1990)102<0322:UPZTAM>2.3.CO;2

Ethier, M. 2001. Re-interpretation of the geology of the Cape Breton Highlands using combined remote sensing and geologic databases. Unpublished MSc thesis, Acadia University, Wolfville, Nova Scotia, 126 p.

Gibson, D., Barr, S.M., van Rooyen, D., White, C.E., and Pilote, J-L. 2021. Protracted intra- and inter-pluton magmatism during the Acadian orogeny: evidence from new LA-ICP-MS U–Pb zircon ages from northwestern Maine, USA. Atlantic Geology, 57, pp. 147–191. https://doi.org/10.4138/atlgeol.2021.008

Grant, C. 2018. Investigating the relationship between the Bras d'Or and Aspy terranes in Cape Breton Island: Insights from Devonian plutonic rocks. Unpublished BSc thesis, Saint Francis Xavier University, Antigonish, Nova Scotia, 60 p.

Grant, C. 2020. Petrological and U–Pb zircon age constraints for metamorphic rocks of the northeastern Cape Breton Highlands, Nova Scotia: New insights into the geological history of the Aspy terrane. Unpublished MSc thesis, Acadia University, Wolfville, Nova Scotia, 244 p.

Grant, C., Archibald, D.B, Kellett, D.A., and Cottle, J.M. 2019. The relationship between the Ganderian Aspy and Bras d'Or terranes explored using Devonian plutonic rocks, Cape Breton, Nova Scotia. *In* Targeted Geoscience Initiative: 2018 report of activities. *Edited by* N. Rogers. Geological Survey of Canada, Open File 8549, pp. 279–286. https://doi.org/10.4095/313659

Hibbard, J.P., van Staal, C.R., Rankin, D.W., and Williams, H. 2006. Lithotectonic map of the Appalachian orogen, Canada - United States of America: Geological Survey of Canada Map 02096A, 2 sheets, scale 1:1 500 000. https://doi.org/10.4095/221912

Hildebrand, R.S. and Whalen, J.B. 2014. Arc and slab-failure magmatism in Cordilleran batholiths II – The Cretaceous Peninsular Ranges Batholith of Southern and Baja California. *In* Stirring the Pot, A Celebration of the Career of Paul F. Hoffman. *Edited by* J.B. Murphy, R.S. Hildebrand, and G.P. Halverson. Geoscience Canada, Reprint Series, 11, pp. 239–267. https://doi.org/10.12789/geocanj.2014.41.059

Horne, R.J., Dunning, G.R., and Jamieson, R.A. 2003. U–Pb age date for the Belle Côte Road orthogneiss, Taylors Barren pluton, and Bothan Brook pluton, southern Cape Breton Highlands (NTS 11K/10, 11K/11): igneous ages and constraints on the age of host and deformational history. *In* Mineral Resources Branch, Report of Activities 2002. *Edited by* D.R. MacDonald.Nova Scotia Department of Natural Resources Re-port 2003-1, pp. 57–68.

Hutchinson, C.S. 1974. Laboratory handbook of Petrographic techniques. Wiley Interscience, New York, 527 p.

Jamieson, R.A., Tallman, P., Marcotte, J.A., Plint, H.E., and Connors, K.A. 1987. Geology of the west-central Cape Breton Highlands, Nova Scotia: Geological Survey of Canada, Paper 87-13, 11 p. https://doi.org/10.4095/122381

Kontak, D.J. and Smith, P.K. 1997. The age and nature of hydrothermal activity effecting auriferous quartz vein mineralization in the Cape Breton Highlands, Nova Scotia. *In* Report of Activities 1996. *Edited by* D. R. MacDonald and K.A. Mills. Nova Scotia Department of Natural Resources, Minerals and Energy Branch, pp. 111–114.

Lin, S. 1994. Relationship between the Aspy and Bras d'Or "terranes" in the northeastern Cape Breton Highlands, Nova Scotia: Reply. Canadian Journal of Earth Sciences, 31, pp.1385–1387. https://doi.org/10.1139/e94-121

Lin, S. 1995. Structural evolution and tectonic significance of the Eastern Highlands shear zone in Cape Breton Island, the Canadian Appalachians: Canadian Journal of Earth Sciences, 32, pp. 545–554. https://doi.org/10.1139/e95-046

Lin, S., Davis, D.W., Barr, S.M., van Staal, C.R., Chen, Y., and Constantin, M. 2007. U–Pb geochronological constraints on the evolution of the Aspy terrane, Cape Breton Island: Implications for relationships between Aspy and Bras d'Or terranes and Ganderia in the Canadian Appalachians. American Journal of Science, 307, pp. 371–398. https://doi.org/10.2475/02.2007.03

Ludwig, K.R. 2012. User's Manual for Isoplot 3.75. A Geological Toolkit for Microsoft Excel. Berkeley Geochronology Center Special Publication, 5, 75 p.

Magyarosi, Z. 2020. Rare-element-enriched pegmatites in central Newfoundland. *In* Current Research (2020). Newfoundland and Labrador Department of Natural Resources. Geological Survey. Report 20-1, pp. 121–143.

Maniar, P.D. and Piccolo, P.M. 1989. Tectonic discriminations of granitoids. Geological Society of America Bulletin, 101, pp. 635–643. https://doi.org/10.1130/0016-7606(1989)101<0635:TDOG>2.3.CO;2

McCarron, T. 2020. Petrology and Geochronology of an inverted metamorphic sequence in the western Cape Breton Highlands, Nova Scotia. Unpublished PhD thesis, University of New Brunswick, Fredericton, New Brunswick, 192 p.

McFarlane, C.R.M. and Luo, Y. 2012. Modern analytical facilities: U–Pb geochronology using 193nm Excimer LA-ICP-MS optimized for in situ accessory mineral dating in thin sections. Geoscience Canada, 39, pp. 158–172.

Miller, B.V., Dunning, G.R., Barr, S.M., Raeside, R.P., Jamieson, R.A., and Reynolds, P.H. 1996. Magmatism and metamorphism in a Grenvillian fragment: U–Pb and $^{40}Ar/^{39}Ar$ ages from the Blair River Complex, northern Cape Breton Island, Nova Scotia, Canada. Geological Society of America Bulletin, 108, pp. 127–140. https://doi.org/10.1130/0016-7606(1996)108<0127:MAMIAG>2.3.CO;2

Paton, C., Hellstrom, J.C., Paul, B., Woodhead, J.D., and Hergt, J.M. 2011. Iolite: Freeware for the visualisation and processing of mass spectrometric data. Journal of Analytical Atomic Spectrometry, 26, pp. 2508–2518. https://doi.org/10.1039/c1ja10172b

Pearce, J.A. 1996. Sources and settings of granitic rocks. Episodes, 19, pp. 120–125. https://doi.org/10.18814/epiiugs/1996/v19i4/005

Pearce, J.A., Harris, N. W. B., and Tindle, A.G. 1984. Trace element discrimination diagrams for the tectonic interpretation of granitic rocks. Journal of Petrology, 25, pp.

956–983. https://doi.org/10.1093/petrology/25.4.956

Peccerillo, A. and Taylor, S.R. 1976. Geochemistry of Eocene calc-alkaline volcanic rocks from the Kastamonu area, northern Turkey. Contributions to Mineralogy and Petrology, 58, pp. 63–81. https://doi.org/10.1007/BF00384745

Petrus, J.A. and Kamber, B.S. 2012. VizualAge: a novel approach to laser ablation ICP-MS U–Pb geochronology data reduction. Geostandards and Geoanalytical Research, 36, pp. 247–270. https://doi.org/10.1111/j.1751-908X.2012.00158.x

Piette-Lauzière, N. 2022. Late Devonian shear zone reactivation in the Canadian Appalachian orogen. Unpublished PhD thesis, University of British Columbia (Okanagan), British Columbia, 621 p.

Piette-Lauzière, N., Larson, K.P., and Kellett, D.A. 2018. Field mapping of the Eastern Highlands shear zone, Cape Breton Island, Nova Scotia. In Targeted Geoscience Initiative, 2017 Report of Activities, Volume 1. *Edited by* N. Rogers. Geological Survey of Canada, Open File 8358, pp. 23–29. https://doi.org/10.4095/306400

Piette-Lauzière, N., Graziani, R., Larson, K.P., and Kellett, D.A. 2019. Reactivation of the Eastern Highlands Shear Zone, Cape Breton Island, Appalachian Orogen. *In* Targeted Geoscience Initiative, 2018 report of activities. *Edited by* N. Rogers; Geological Survey of Canada, Open File 8549, pp. 295–305. https://doi.org/10.4095/313663

Piette-Lauzière, N., Larson, K.P., Kellett, D.A., Rogers, N. and Powell, J. in press. Late Devonian shear zone reactivation in the Canadian Appalachian orogen. Geological Society, London, Special Publications. https://doi.org/10.1144/SP542-2022-350

Price, J., Barr, S.M., Raeside, R.P., and Reynolds, P. 1999. Petrology, tectonic setting, and $^{40}Ar/^{39}Ar$ (hornblende) dating of the Late Ordovician–Early Silurian Belle Cote Road orthogneiss, western Cape Breton Highlands, Nova Scotia. Atlantic Geology, 35, pp. 1–17. https://doi.org/10.4138/2021

Raeside, R. P. and Barr, S. M. 1992. Geology of the northern and eastern Cape Breton Highlands, Nova Scotia. Geological Survey of Canada. Paper 89–14, 39p. https://doi.org/10.4095/134060

Smith, A.M. 2022. Petrology, tectonic setting, and critical element potential of the Park Spur pluton, Aspy terrane, Cape Breton Highlands, Nova Scotia. Unpublished BSc thesis, Acadia University, Wolfville, Nova Scotia, 113p.

Sombini dos Santos, G., Barr, S.M., White, C.E., and van Rooyen, D. 2020. The rapakivi-bearing Margaree pluton, Cape Breton Island, Canada: Evidence for a Late Devonian post-tectonic cryptic silicic-mafic magma chamber. Canadian Journal of Earth Sciences, 57, pp. 1011–1029. https://doi.org/10.1139/cjes-2019-0220

Streckeisen, A. 1976. To each plutonic rock its proper name. Earth Sciences Reviews, 12, pp. 1–33. https://doi.org/10.1016/0012-8252(76)90052-0

Sun, S. and McDonough, W.F. 1989. Chemical and isotopic systematic of oceanic basalts: implications for mantle composition and processes. *In* Geological Society of London, Special Publications 42, pp. 313–345. https://doi.org/10.1144/GSL.SP.1989.042.01.19

Sunatori, E. 2022. Extent and timing of deformation and metamorphism associated with the Eastern Highlands Shear Zone, central Cape Breton Highlands, Nova Scotia. Unpublished MSc thesis, Acadia University, Wolfville, Nova Scotia, 358 p.

Van Rooyen, D. and Barr, S.M. 2020. Ages of plutons associated with economic mineralization in Cape Breton Island, Nova Scotia. *In* Geoscience and Mines Branch, Report of Activities 2019–2020. *Edited by* E.W. MacDonald and D.R. MacDonald. Nova Scotia Department of Energy and Mines, Report ME 2020-002, pp. 123–129.

Van Rooyen, D. and Barr, S.M. 2022. Ages of plutons associated with economic mineralization in Cape Breton Island, Nova Scotia. Nova Scotia Mineral Resources Development Fund Research Grant 2019-030; Open File Report ME 2022-34, 3 p.

Van Staal, C.R. and Barr, S.M. 2012. Lithospheric architecture and tectonic evolution of the Canadian Appalachians. *In* Tectonic Styles in Canada Revisited: the LITHOPROBE perspective. *Edited by* J.A. Percival, F.A. Cook, and R.M. Clowes. Geological Association of Canada, Special Paper 49, pp. 41–95.

Van Staal, C.R., Whalen, J.B., Valverde-Vaquero, P., Zagorevski, A., and Rogers, N. 2009. Pre- Carboniferous, episodic accretion-related, orogenesis along the Laurentian margin of the northern Appalachians. *In* Ancient Orogens and Modern Analogues. *Edited by* J.B. Murphy, J. D. Keppie, and A.J. Hynes. Geological Society, London, Special Publication 327, pp. 271–316. https://doi.org/10.1144/SP327.13

Van Staal, C.R., Barr, S.M., Waldron, J.W.F., Schofield, D.I., Zagorevski, A., and White, C.E. 2021. Provenance and Paleozoic tectonic evolution of Ganderia and its relationships with Avalonia and Megumia in the Appalachian-Caledonide orogen. Gondwana Research, 98, pp. 212–243. https://doi.org/10.1016/j.gr.2021.05.025

Waldron, J.W.F., Barr, S.M., Park, A., and White, C.E. 2015. Late Paleozoic strike-slip reconfiguration of the northern Appalachians. Tectonics, 34, 1661–1684. https://doi.org/10.1002/2015TC003882

Whalen, J. B., Currie, K. L., and Chappell, B. W. 1987. A-type granites: Geochemical characteristics, discrimination and petrogenesis. Contributions to Mineralogy and Petrology, 95, pp. 407–419. https://doi.org/10.1007/BF00402202

White, C.E., Sombini dos Santos, G., Moning, A.A., Barr, S.M., and van Rooyen, D. 2018. Geological and geochronological studies in the Middle River–Leonard MacLeod Brook area, central Cape Breton Island, Nova Scotia. *In* Geoscience and Mines Branch, Report of Activities 2016. *Edited by* E.W. MacDonald and D.R. MacDonald. Nova Scotia Department of Natural Resources, Report ME 2018-001, pp. 89–97.

White, C.E., Barr, S.M., and Raeside, R.P. 2022. Geological Journey Map of Nova Scotia, Fourth Edition. Atlantic

Geoscience Society Special Publication # 64, scale 1:610 000.

Yaowanoiyothin, W. 1988. Petrology of the Black Brook Granitic Suite and associated gneiss, northeastern Cape Breton Highlands, Nova Scotia. Unpublished MSc thesis, Acadia University, Wolfville, Nova Scotia, 321 p.

Yaowanoiyothin, W. and Barr, S.M. 1991. Petrology of the Black Brook Granitic Suite, Cape Breton Island, Nova Scotia. Canadian Mineralogist, 29, pp. 499–515.

Editorial responsibility: David P. West, Jr.